

- We propose four new large-scale datasets for one-shot relational learning in TKGs. For every long-tail relation, we have a substantial number of associated TKG facts, which greatly alleviates instability in model training and evaluation.
- We fix the unfair evaluation settings employed by previous KG FSL methods, and report comprehensive evaluation results on our datasets.
- We propose a model solving both interpolated and extrapolated LP tasks for one-shot relations in TKGs, and evaluate our model on all four newly-proposed datasets. Our model achieves state-of-the-art performance on all datasets in both LP tasks while keeping a low time cost.

2 Related Work

KG representation learning has brought success to KG models in recent years. A line of methods are translational models (Bordes et al., 2013; Lin et al., 2015; Sun et al., 2019; Abboud et al., 2020), while another series of methods are based on tensor factorization (Nickel et al., 2011; Yang et al., 2015; Balazevic et al., 2019). On top of them, neural-based models (Schlichtkrull et al., 2018; Vashishth et al., 2020) incorporates deep learning into these two lines of models and achieve strong performance. To further model temporal dynamics of TKGs, a number of studies have been conducted (Leblay and Chekol, 2018; Ma et al., 2019; Lacroix et al., 2020; Jin et al., 2020; Wu et al., 2020; Han et al., 2021b,a; Jung et al., 2021; Ding et al., 2021), and have shown great effectiveness.

Xiong et al. (Xiong et al., 2018) find that data scarcity problem exists in KGs and traditional KG representation learning methods fail to model sparse KG relations. To solve this problem, several researches (Xiong et al., 2018; Chen et al., 2019; Zhang et al., 2020; Sheng et al., 2020; Niu et al., 2021) employ FSL paradigm (Vinyals et al., 2016; Sung et al., 2018) and make improvement in learning sparse relations. Mirtaheri et al. (Mirtaheri et al., 2021) find the same problem in TKGs and develop a one-shot TKG reasoning model aiming to better model sparse relations in TKGs. Please refer to Appendix A for more details.

3 Task Formulation

Let \mathcal{E} , \mathcal{R} and \mathcal{T} represent a finite set of entities, relations and timestamps, respectively. A temporal knowledge graph \mathcal{G} is a relational graph consisting of a finite set of facts denoted with quadruples in the form of (s, r, o, t) , i.e., $\mathcal{G} = \{(s, r, o, t) | s, o \in \mathcal{E}, r \in \mathcal{R}, t \in \mathcal{T}\}$. We define the TKG link prediction (LP) tasks as follows. A complete TKG contains both the observed facts and the unobserved true facts, i.e., $\mathcal{G} = \{\mathcal{G}_{obs}, \mathcal{G}_{un}\}$. Given \mathcal{G}_{obs} , TKG LP aims to predict the ground truth object (or subject) entities of queries $(s, r, ?, t)$ (or $(?, r, o, t)$), where $(s, r, o, t) \in \mathcal{G}_{un}$. For any link prediction query $(s, r, ?, t_q)$ (or $(?, r, o, t_q)$), while in the interpolation task the prediction can be based on all the observed facts $\{(s, r, o, t_i) | t_i \in \mathcal{T}\}$ from any timestamp, the extrapolated LP task further regulates that the prediction can only be based on the observed past facts $\{(s, r, o, t_i) | t_i < t_q\}$. In our work, we only consider object prediction since we add reciprocal relations for every quadruple, i.e., adding (o, r^{-1}, s, t) for every (s, r, o, t) . The restriction to only predict object entities does not lead to a loss of generality.

3.1 One-shot Temporal Knowledge Graph Link Prediction Setup

TKG LP can be generalized to the one-shot setting as follows. Given a TKG \mathcal{G} , all its relations \mathcal{R} can be classified into two groups, i.e., frequent relations \mathcal{R}_{freq} and sparse relations \mathcal{R}_{sp} . Following the standard KG one-shot learning setting (Xiong et al., 2018; Mirtaheri et al., 2021), we assume that we have access to a set of training tasks. Each training task T_r corresponds to a sparse KG relation $r \in \mathcal{R}_{sp}^{train}$ ($\mathcal{R}_{sp}^{train} \subset \mathcal{R}_{sp}$). $T_r = \{\mathcal{S}_r, \mathcal{Q}_r\}$, where $\mathcal{S}_r = \{(s_0, r, o_0, t_0)\}$ is a set containing only one support quadruple (s_0, r, o_0, t_0) , and $\mathcal{Q}_r = \{(s_q, r, o_q, t_q) | s_q, o_q \in \mathcal{E}, t_q \in \mathcal{T}\} \setminus \{(s_0, r, o_0, t_0)\}$ is a set containing the rest of quadruples concerning the sparse relation r . We name \mathcal{S}_r and \mathcal{Q}_r as the support set and the query set of the task T_r , respectively. And the set of all training tasks is also denoted as the meta-training set $\mathbb{T}_{meta-train}$ ($\mathbb{T}_{meta-train} = \{T_r | r \in \mathcal{R}_{sp}^{train}\}$). For every sparse relation r , the goal of one-shot TKG LP is to accurately predict the missing entities of all the LP queries $(s_q, r, ?, t_q)$ (or $(?, r, o_q, t_q)$) derived from query quadruples $(s_q, r, o_q, t_q) \in \mathcal{Q}_r$, with only one observed r -specific support quadruple (s_0, r, o_0, t_0) from \mathcal{S}_r . After the meta-training

process, TKG reasoning models will be evaluated on meta-test tasks $\mathbb{T}_{meta-test}$ corresponding to unseen sparse relations \mathcal{R}_{sp}^{test} , where $\mathcal{R}_{sp}^{test} \subset \mathcal{R}_{sp}$ and $\mathcal{R}_{sp}^{train} \cap \mathcal{R}_{sp}^{test} = \emptyset$. We also validate the model performance with a meta-validation set $\mathbb{T}_{meta-valid}$ ($\mathcal{R}_{sp}^{valid} \subset \mathcal{R}_{sp}$, $\mathcal{R}_{sp}^{train} \cap \mathcal{R}_{sp}^{valid} = \emptyset$, $\mathcal{R}_{sp}^{valid} \cap \mathcal{R}_{sp}^{test} = \emptyset$). Similar to meta-training, for each sparse relation in meta-validation and meta-test, only one associated quadruple is observed in its support set, and all the links in its query set are to be predicted. Besides, same as (Xiong et al., 2018; Mirtaheri et al., 2021), a background graph $\mathcal{G}' = \{(s, r, o, t) | s, o \in \mathcal{E}, r \in \mathcal{R}_{freq}, t \in \mathcal{T}\}$ is constructed by including all the quadruples concerning frequent relations, and it is also observable to the TKG reasoning model.

For each sparse relation r , in the interpolated LP, there is no constraint for the timestamp t_0 of its support quadruple (s_0, r, o_0, t_0) , while in the extrapolated LP, temporal constraint is imposed that $t_0 < \min(\{t_q | (s_q, r, o_q, t_q) \in \mathcal{Q}_r\})$. Moreover, in the interpolated LP, we assume that the whole background graph is always observable, while in the extrapolated LP, only the background graph before the one-shot support quadruple is observable. Following the extrapolation setting in (Mirtaheri et al., 2021), we keep the time span of meta-learning sets ($\mathbb{T}_{meta-train}$, $\mathbb{T}_{meta-valid}$, $\mathbb{T}_{meta-test}$) in a non-overlapped sequential order (Figure 4).

4 Our Method

Figure 1 shows the overview of MOST. MOST consists of two components: (1) Time-aware relational graph encoder for learning contextualized time-aware entity representations; (2) Meta-relational decoder employed to generate meta representations for sparse relations and compute the plausibility scores of the quadruples.

4.1 Time-aware Relational Graph Encoder

MOST employs a time-aware relational graph encoder to learn the contextualized entity representations of support entities. For every support entity e , MOST first finds e 's temporal neighbors. It searches for the background facts whose object entity corresponds to e , and constructs a temporal neighborhood, i.e., $\mathcal{N}_e = \{(e', r', t') | r' \in \mathcal{R}_{freq}, (e', r', e, t') \in \mathcal{G}'\}$. To avoid including excessive noisy information, MOST filters these background facts and only keeps a fixed number of temporal neighbors nearest to the timestamp of

the support quadruple t_0 (MOST ensures the kept neighbors are prior to t_0 for extrapolated LP). The number of sampled neighbors is a hyperparameter and can be tuned. We denote the filtered neighborhood as $\tilde{\mathcal{N}}_e$.

MOST then computes e 's time-aware representation by aggregating the information provided by its temporal neighbors. Inspired by (Vashishth et al., 2020), our relational graph encoder derives the entity representations as follows:

$$\begin{aligned} \tilde{\mathbf{h}}_e^{l+1} &= \frac{1}{|\tilde{\mathcal{N}}_e|} \sum_{(e', r', t') \in \tilde{\mathcal{N}}_e} \mathbf{W}^l (f(\mathbf{h}_{e'}^l \parallel \Phi(t')) \circ \mathbf{h}_{r'}), \\ \mathbf{h}_e^{l+1} &= \mathbf{h}_e^l + \delta_1 \sigma(\tilde{\mathbf{h}}_e^{l+1}). \end{aligned} \quad (1)$$

$\tilde{\mathbf{h}}_e^{l+1}$ denotes e 's entity representation in the $(l+1)^{th}$ layer. $\mathbf{h}_{r'}$ denotes the relation representation of the frequent relation r' . Moreover, \circ, \parallel represent Hadamard product and concatenation operation, respectively. \mathbf{W}^l is a weight matrix that processes the information in the l^{th} layer. f is a layer of feed-forward neural network. δ_1 is a trainable parameter deciding how much temporal information is included in updating entity representation. $\sigma(\cdot)$ is an activation function. $\Phi(t')$ denotes the time encoding function that encodes timestamp t' as: $\sqrt{\frac{1}{d_t}} [\cos(\omega_1 t' + \phi_1), \dots, \cos(\omega_{d_t} t' + \phi_{d_t})]$, where d_t is the dimension of the time representation, $\omega_1 \dots \omega_{d_t}$ and $\phi_1 \dots \phi_{d_t}$ are trainable parameters. We name our model with this timestamp encoder as MOST-TA. Due to the success of (Xu et al., 2020) who encodes time differences for dynamic graphs, we input $t_0 - t'$ instead of t' into the time encoder $\Phi(\cdot)$ and derive another model variant MOAT-TD. We show in experiments (Section 5.3) that both MOST-TA and MOST-TD can achieve state-of-the-art performance in one-shot TKG LP tasks.

4.2 Meta-relational Decoder

Assume we have a meta-learning task T_r , and we have a support quadruple $(s_0, r, o_0, t_0) \in \mathcal{S}_r$, with several query quadruples $(s_q, r, o_q, t_q) \in \mathcal{Q}_r$. After obtaining the time-aware representations for support entities, i.e., \mathbf{h}_{s_0} and \mathbf{h}_{o_0} , we learn a meta representation for the sparse relation r :

$$\mathbf{h}_r = \text{MLP}(\mathbf{h}_{s_0} \parallel \mathbf{h}_{o_0}), \quad (2)$$

where MLP is a multilayer perceptron consisting of three layers of feed-forward neural network.

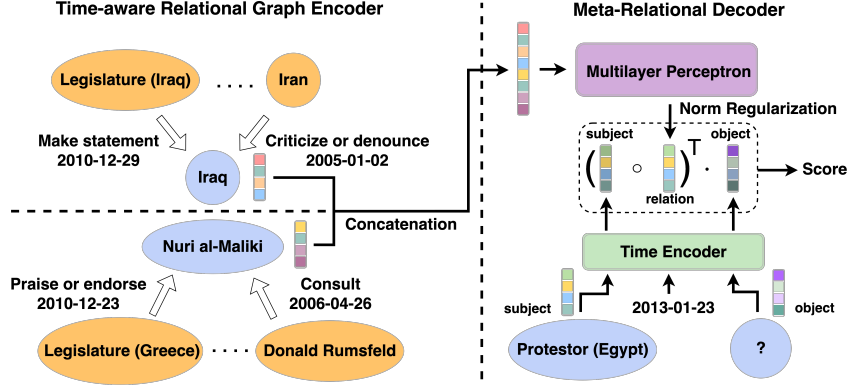


Figure 1: Overview of MOST. Assume we have a sparse relation *Appeal for change in leadership* and the associated support quadruple is $(Iraq, \textit{Appeal for change in leadership}, Nuri\ al\ Maliki, 2013-01-15) \in \mathcal{S}_r$. MOST first finds the nearest observable temporal neighbors of support entities, i.e., *Iraq* and *Nuri al-Maliki*, and computes their contextualized time-aware representations. Concatenated support entity representations are then through a multilayer perceptron, which generates a meta-representation for the sparse relation. Assume we have a query quadruple $(Protector\ (Egypt), \textit{Appeal for change in leadership}, Head\ of\ Government\ (Egypt), 2013-01-23) \in \mathcal{Q}_r$ and it derives a link prediction query $(Protector\ (Egypt), \textit{Appeal for change in leadership}, ?, 2013-01-23)$. Candidate entity representations are updated with a time encoder and the scoring function will compute the plausibility scores of the quadruples with different candidates.

For a link prediction query $(s_q, r, ?, t_q)$ (generated from a query quadruple (s_q, r, o_q, t_q)), we compute the time-aware representations of s_q as well as every candidate entity as follows:

$$\mathbf{h}_e^{l+1} = \mathbf{h}_e^l + \delta_2 f(\mathbf{h}_e^l \| \Phi(t_q)). \quad (3)$$

δ_2 is a trainable parameter controlling the amount of the injected temporal information. We do not search temporal neighbors for every candidate entity to avoid huge time consumption. Similarly, MOST-TD adapts Equation 3 to the following form to enable time difference learning:

$$\mathbf{h}_e^{l+1} = \mathbf{h}_e^l + \delta_2 f(\mathbf{h}_e^l \| \Phi(t_q - t_0)). \quad (4)$$

Inspired by (Sun et al., 2019), we map the entity representations to the complex space, and treat the meta representations of sparse relations as element-wise rotation. We use the following scoring function to compute the scores regarding different candidates e_c :

$$\Psi_{e_c}^r = \frac{1}{1 + \exp\left(-\left(\mathbf{h}_{s_q} \circ \tilde{\mathbf{h}}_r\right)^T \mathbf{h}_{e_c}\right)} \quad (5)$$

$\tilde{\mathbf{h}}_r = \frac{1}{\|\mathbf{h}_r\|_\infty} \mathbf{h}_r$, and $\|\mathbf{h}_r\|_\infty$ denotes the infinity norm of the vector \mathbf{h}_r . In our framework, the meta representations of sparse relations are computed from the one-shot support entity representations, thus naturally coupled with noise. We adaptively

regularize the lengths of meta representations by dividing themselves by their infinity norm. We do not divide by L2 norm since we argue that both the directions and the lengths of meta representations contribute to prediction. Diving by L2 norm will lose length information. We name this process as norm regularization.

4.3 Parameter Learning

We use the binary cross entropy loss to train our model. The loss function in our work is in the following form:

$$l_q^{e_c} = y_q^{e_c} \log \Psi_{e_c}^r + (1 - y_q^{e_c})(1 - \log \Psi_{e_c}^r),$$

$$\mathcal{L} = - \sum_{r \in \mathcal{R}_{sp}^{train}} \frac{1}{2|\mathcal{Q}_r|} \sum_q \frac{1}{|\mathcal{E}|} \sum_{e_c \in \mathcal{E}} l_q^{e_c}. \quad (6)$$

q denotes a LP query derived from the query quadruple $(s_q, r, o_q, t_q) \in \mathcal{Q}_r$ corresponding to a sparse relation $r \in \mathcal{R}_{sp}^{train}$. $y_q^{e_c}$ is the binary label indicating whether a candidate entity e_c is the ground truth missing entity from q or not. Note that in Equation 6, for every query quadruple q , we average the loss over all the entities $e_c \in \mathcal{E}$ other than o_q (or s_q), rather than sampling a fixed number of negative samples as in previous KG FSL methods (Xiong et al., 2018; Chen et al., 2019; Zhang et al., 2020; Niu et al., 2021; Mirtaheri et al., 2021).

5 Experiments

We evaluate MOST on both interpolated and extrapolated TKG LP in the one-shot setting. We propose four new large-scale datasets and evaluate previous KG FSL methods on them.

5.1 Datasets

Dataset	$ \mathcal{E} $	$ \mathcal{R} $	$ \mathcal{T} $	$ \mathbb{T} $
ICEWS05-15-one_ext	7,934	109	4,017	53/6/11
ICEWS05-15-one_int	10,356	155	4,017	74/9/10
GDELTONe_ext	6,647	155	2,751	55/7/11
GDELTONe_int	7,677	181	2,751	64/8/8

Table 1: Dataset statistics. $|\mathbb{T}|$ denotes the number of meta-learning tasks in $\mathbb{T}_{meta-train}$, $\mathbb{T}_{meta-valid}$, $\mathbb{T}_{meta-test}$.

By taking subsets of two benchmark TKG databases, i.e., ICEWS (Boschee et al., 2015) and GDELTONe (Leetaru and Schrodte, 2013), Mirtaheri et al. (Mirtaheri et al., 2021) propose two one-shot extrapolation LP datasets, i.e., ICEWS17 and GDELTONe. They first set upper and lower thresholds, and then select the relations with frequency between them as sparse relations (frequency 50 to 500 for ICEWS17, 50 to 700 for GDELTONe). To prevent time overlaps among meta-learning sets ($\mathbb{T}_{meta-train}$, $\mathbb{T}_{meta-valid}$, $\mathbb{T}_{meta-test}$), they further remove a significant number of quadruples regarding sparse relations. For example, a relation r is selected as a sparse relation and $T_r \in \mathbb{T}_{meta-train}$. The ending timestamp of the meta-training set is t' . Then all the quadruples in $\{(s, r, o, t) | s, o \in \mathcal{E}, t > t'\}$ are removed from the dataset. This leads to a considerably smaller query set Q_r when a large number of r -related events take place after t' . If r 's frequency is close to the lower threshold before removal, it is very likely that after removal, the number of associated quadruples left in $\{(s, r, o, t) | s, o \in \mathcal{E}, t \leq t'\}$ becomes extremely small, leading to a tiny query set Q_r that causes instability during training. Similarly, if $T_r \in \mathbb{T}_{meta-valid}$ or $T_r \in \mathbb{T}_{meta-test}$, evaluation on a tiny query set Q_r makes it hard to accurately determine the performance of the model since the test data is not comprehensive. As shown in Figure 2, a large portion of sparse relations in ICEWS17 and GDELTONe have very few associated quadruples, which introduces instability in model training and evaluation.

To overcome this problem, we construct two new large-scale extrapolation LP datasets, i.e., ICEWS-one_ext and GDELTONe_ext, also by tak-

ing subsets from ICEWS (Boschee et al., 2015) and GDELTONe (Leetaru and Schrodte, 2013). ICEWS-one_ext contains timestamped political facts happening from 2005 to 2015, while GDELTONe_ext contains global social facts from Jan. 1, 2018 to Jan. 31, 2018. For sparse relation selection, we set the upper and lower thresholds of frequency to 100 and 1000 for ICEWS-one_ext, 200 and 2000 for GDELTONe_ext, and then split these relations into train/valid/test groups. We take the relations with higher frequency as frequent relations \mathcal{R}_{freq} and build background graphs \mathcal{G}' with all the quadruples containing them. Following (Mirtaheri et al., 2021), we then remove a part of quadruples associated with sparse relations to prevent time overlaps among meta-learning sets. After removal, we further discard the relations with too few associated quadruples (less than 50 for ICEWS-one_ext, 100 for GDELTONe_ext). In this way, we prevent including meta-tasks T_r with extremely small query set Q_r . From Figure 2, we observe that ICEWS-one_ext and GDELTONe_ext have a substantial number of associated quadruples for each sparse relation, which greatly alleviates instability in model training and evaluation.

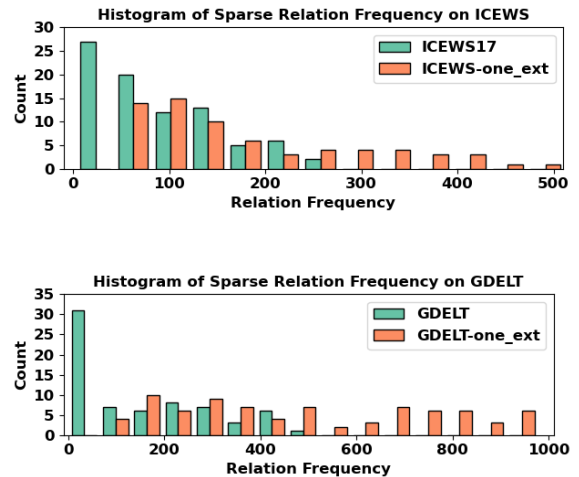


Figure 2: Sparse Relation frequency comparison between ICEWS-one_ext and ICEWS17; GDELTONe_ext and GDELTONe.

Similarly, we construct two more datasets, i.e., ICEWS-one_int and GDELTONe_int, for interpolated LP in the one-shot setting. Since in interpolated LP, there exists no constraint on the support timestamp t_0 , we do not have to remove quadruples to eliminate time overlaps among meta-learning sets. To this end, we set the upper and lower thresh-

olds of sparse relations’ frequency to 50 and 500 for ICEWS-one_int, 100 and 1000 for GDELT-one_int, and then split these relations into train/valid/test groups. Statistics of our datasets are presented in Table 1 and we provide more details about data construction in Appendix J.

5.2 Baseline Methods

We compare our model with two groups of baseline methods on both interpolated and extrapolated LP in the one-shot setting.

Few-shot Relational Learning Methods

We consider five static KG FSL methods, i.e., Gmatching (Xiong et al., 2018), MetaR (Chen et al., 2019), FSRL (Zhang et al., 2020), FAAN (Sheng et al., 2020), GANA (Niu et al., 2021), and a TKG FSL method, i.e., OAT (Mirtaheri et al., 2021). In (Mirtaheri et al., 2021), static KG FSL methods are trained and evaluated on an unweighted static KG derived from collapsing the original TKG, which greatly decreases the inductive bias brought by the original TKG and causes poor performance of these methods. In our work, we provide static KG FSL methods with all the facts in the original datasets, and neglect time information, i.e., neglecting t in (s, r, o, t) . We provide a detailed explanation and prove our assertion empirically with further experiments in Appendix E.

Temporal Knowledge Graph Embedding Methods

Three TKG interpolation methods, i.e., TNTComplEx (Lacroix et al., 2020), ATiSE (Xu et al., 2019), TeLM (Xu et al., 2021), and three TKG extrapolation methods, i.e., TANGO (Han et al., 2021b), CyGNet (Zhu et al., 2021), xERTE (Han et al., 2021a) are selected as our baselines. For each interpolation dataset, we build a training set for these methods by adding all the quadruples of the background graph \mathcal{G}' and the quadruples associated with all the meta-training relations \mathcal{R}_{sp}^{train} . We further add the support quadruple associated with each sparse relation $r \in \{\mathcal{R}_{sp}^{valid}, \mathcal{R}_{sp}^{test}\}$ into the training set. For each extrapolation dataset, we build a training set by adding all the background quadruples during meta-training time \mathcal{G}'_{train} , as well as all the quadruples concerning every $r \in \mathcal{R}_{sp}^{train}$. We do not include any quadruple regarding $r \in \{\mathcal{R}_{sp}^{valid}, \mathcal{R}_{sp}^{test}\}$ into the training set due to the time constraint in the extrapolation setting. But we allow the models to have access to the support quadruples

$(\mathcal{S}_r, r \in \{\mathcal{R}_{sp}^{valid}, \mathcal{R}_{sp}^{test}\})$ during inference. We test TKG embedding baselines with the same quadruples tested by FSL methods to ensure fair comparison.

5.3 Experimental Results

Previous KG FSL methods only report object prediction results. To achieve comprehensive results, for each test quadruple (s_q, r_q, o_q, t_q) , we derive two LP queries, i.e., $(s_q, r_q, ?, t_q)$ and $(?, r_q, o_q, t_q)$, and perform prediction on both of them. We employ two evaluation metrics, i.e., Hits@1/3/5/10 and mean reciprocal rank (MRR), to evaluate model performance in all experiments. We also follow (Bordes et al., 2013) and use filtered results for fairer evaluation. More details of evaluation protocol are provided in Appendix C.

Table 2 and Table 3 report the experimental results of one-shot interpolated and extrapolated LP, respectively. We find that static KG FSL methods can achieve competitive or even better performance compared with traditional TKG embedding methods, implying the effectiveness of FSL in modeling sparse relations in KGs. MOST outperforms baseline methods on all datasets in both LP tasks. While MOST-TA performs better than MOST-TD in the interpolation task, MOST-TD outperforms MOST-TA in predicting future facts. This can be explained as follows. In the interpolated LP, part of the TKG at every timestamp is observable during training, thus enabling the time encoder to learn from all the timestamps. However, in the extrapolated LP, meta-training set does not span across the whole timeline, which leads to the degenerated model performance during inference when we sample the temporal neighbors from the timestamps unseen in the meta-training set. For extrapolation, modeling time differences achieves better results since almost all time differences we encounter during inference are already seen and learned during meta-training.

5.4 Ablation Study

To validate the effectiveness of model components, we derive model variants for both MOST-TA and MOST-TD, and conduct several ablation studies on ICEWS-one_int and ICEWS-one_ext. We present the experimental results in Table 4 and Table 5. We devise model variants from the following angles:

(A) Temporal Neighbor Sampling Strategy:

In A1, we keep all the temporal neighbors, without limiting the size of the sampled neighborhood. In A2, we still keep a fixed number of temporal

Datasets	ICEWS-one_int					GDELT-one_int				
Model	MRR	Hits@1	Hits@3	Hits@5	Hits@10	MRR	Hits@1	Hits@3	Hits@5	Hits@10
TNTComplEx	23.34	14.57	27.21	31.54	36.88	11.95	6.76	11.98	15.58	21.78
ATiSE	34.40	22.03	39.51	49.25	60.57	7.77	5.10	6.72	8.13	12.13
TeLM	35.38	24.42	39.21	47.74	59.12	10.41	5.97	10.37	13.28	18.87
GANa	13.83	6.07	19.21	24.00	27.23	5.89	2.53	6.54	8.35	12.20
MetaR	27.69	7.88	41.02	52.58	61.78	9.91	0.18	14.61	19.62	26.79
GMatching	30.59	15.46	39.33	48.80	58.62	12.53	6.55	12.80	17.14	24.15
FSRL	33.98	18.94	44.48	52.61	59.82	14.11	7.61	14.67	19.56	27.54
FAAN	35.48	23.27	43.36	49.45	57.73	14.77	7.67	16.19	21.35	27.11
OAT	11.55	5.47	10.09	14.81	23.42	12.28	7.70	12.59	15.18	21.47
MOST-TA	47.79	39.91	51.79	57.01	62.25	17.71	11.56	19.07	23.25	29.76
MOST-TD	47.60	39.43	51.98	56.83	62.38	17.36	11.67	18.18	22.74	28.63

Table 2: Interpolated LP results for one-shot relational learning on ICEWS-one_int and GDELT-one_int. Evaluation metrics are filtered MRR and Hits@1/3/5/10. The best results are marked in bold. More discussions in Appendix F.

Datasets	ICEWS-one_ext					GDELT-one_ext				
Model	MRR	Hits@1	Hits@3	Hits@5	Hits@10	MRR	Hits@1	Hits@3	Hits@5	Hits@10
TANGO	10.23	3.94	11.40	15.88	25.78	13.88	9.61	13.17	16.93	22.29
CyGNet	22.30	12.61	25.51	30.46	39.13	9.42	4.87	9.74	13.13	16.81
xERTE	30.02	19.79	36.63	42.13	51.16	16.38	10.88	18.23	22.19	27.76
GANa	11.34	3.70	15.52	19.25	25.67	7.12	4.85	7.02	8.89	11.13
MetaR	23.50	9.01	32.95	40.18	48.73	9.66	0.03	13.79	19.52	26.30
GMatching	20.30	12.35	21.06	28.80	38.02	12.26	8.41	11.44	13.76	19.01
FSRL	18.06	12.09	17.68	21.06	32.23	6.96	2.52	8.81	11.58	14.13
FAAN	25.73	15.86	29.14	35.95	43.73	14.36	8.71	15.31	18.46	23.71
OAT	9.24	7.02	7.31	7.40	11.88	14.06	6.71	13.43	18.59	28.11
MOST-TA	32.94	26.35	34.64	39.97	47.19	15.69	10.14	16.49	20.54	26.38
MOST-TD	38.46	31.51	40.73	46.02	52.32	17.36	11.64	18.37	22.46	28.15

Table 3: Extrapolated LP results for one-shot relational learning on ICEWS-one_ext and GDELT-one_ext. Evaluation metrics are filtered MRR and Hits@1/3/5/10. The best results are marked in bold. More discussions in Appendix F.

Datasets	ICEWS-one_int			ICEWS-one_ext		
Variants	MRR	Hits@1	Hits@10	MRR	Hits@1	Hits@10
A1	46.22	37.04	62.20	31.75	23.85	45.55
A2	45.85	37.22	61.88	32.03	24.36	47.16
B1	46.15	37.86	62.23	31.66	23.05	47.07
B2	11.75	6.14	23.62	11.40	4.86	25.80
B3	16.27	7.36	32.47	26.13	17.97	43.65
C1	43.15	32.81	62.22	31.77	24.74	44.16
C2	42.81	31.52	62.10	32.34	26.01	45.60
MOST-TA	47.79	39.91	62.25	32.94	26.35	47.19

Table 4: Ablation studies of MOST-TA variants on ICEWS-one_int and ICEWS-one_ext. The best results are marked in bold.

Datasets	ICEWS-one_int			ICEWS-one_ext		
Variants	MRR	Hits@1	Hits@10	MRR	Hits@1	Hits@10
A1	44.01	35.40	60.89	35.96	28.63	49.83
A2	43.77	33.81	62.25	35.89	29.01	50.25
B1	42.94	32.02	62.28	36.30	29.52	51.22
B2	11.78	6.21	23.44	11.67	4.78	24.78
B3	23.68	13.87	44.40	27.35	18.82	43.78
C1	41.06	29.04	62.25	36.81	30.24	50.16
C2	43.33	32.96	62.36	36.84	29.52	50.67
MOST-TD	47.60	39.43	62.38	38.46	31.51	52.32

Table 5: Ablation studies of MOST-TD variants on ICEWS-one_int and ICEWS-one_ext. The best results are marked in bold.

neighbors, but we randomly sample them instead of keeping the nearest ones. We observe that by sampling nearest neighbors, we exclude excessive noise from farther neighbors and achieve better

results.

(B) Decoder Variants: In B1, we switch the infinity norm to the L2 norm during norm regularization. In B2, we take the raw entity repre-

sentations of query entities as the input into our decoder, without injecting temporal information through Equation 3 and Equation 4. In B3, we employ the LSTM-based matcher (Hochreiter and Schmidhuber, 1997) proposed in (Xiong et al., 2018) instead of the scoring function (Equation 5) in our meta-relational decoder. We observe that dividing by infinity norms helps to adaptively regularize the lengths of meta representations and improve model performance. Compared with (Xiong et al., 2018), our meta-relational decoder employs a stronger scoring function. During score computation, introducing temporal information into the query entities greatly increases performance.

(C) **Graph Encoder Variants:** In C1, we use RGCN (Schlichtkrull et al., 2018) instead of our graph encoder. In C2, we remove time encoder $\Phi(\cdot)$ during aggregation in our graph encoder. We observe that incorporating temporal information into the graph encoder helps to improve model performance.

5.5 Performance over Different Relations

We report the model performance over every sparse relation in ICEWS-one_int (Table 6) and ICEWS-one_ext (Table 7). We compare MOST with the strongest FSL baseline FAAN. Experimental results show that MOST achieves performance gain in all sparse relations, which implies its robustness.

ICEWS-one_int		MRR		Hits@10	
CAMEO	Frequency	MOST-TA	FAAN	MOST-TA	FAAN
1313	65	35.25	28.13	57.03	46.09
1411	89	53.65	40.86	71.02	67.61
035	92	50.50	36.38	71.42	63.73
151	118	75.75	53.06	85.04	82.47
023	146	52.69	49.37	64.48	63.10
191	175	63.83	49.41	75.57	75.28
1721	282	38.45	34.33	51.24	53.20
015	269	39.54	25.66	53.17	48.50
064	349	29.75	15.18	47.12	34.48
128	436	57.84	43.37	71.95	72.52

Table 6: Performance over each sparse relation in ICEWS-one_int. CAMEO denotes the CAMEO code for each relation. The best results are marked in bold.

5.6 Time Cost Analysis

We report in Figure 3 and Table 8 the time cost of MOST and several strong baselines on both ICEWS-based datasets. We observe that MOST achieves the best performance on LP tasks while keeping a low time cost. Though MOST-TD and MOST-TA achieve weaker performance than their

ICEWS-one_ext		MRR		Hits@10	
CAMEO	Frequency	MOST-TD	FAAN	MOST-TD	FAAN
074	55	32.85	17.63	57.40	24.07
1122	57	21.39	4.99	29.46	13.39
0241	65	22.05	21.60	35.15	32.81
015	67	26.31	23.30	42.42	38.63
064	93	30.41	18.52	50.00	44.02
113	107	21.67	15.40	33.96	31.13
033	127	37.13	28.26	53.96	53.17
0214	128	42.91	43.88	55.11	52.36
072	130	33.51	9.74	47.28	32.17
154	180	59.61	32.96	72.06	65.64
115	184	47.47	36.28	61.20	54.09

Table 7: Performance over each sparse relation in ICEWS-one_ext. CAMEO denotes the CAMEO code for each relation. The best results are marked in bold.

counterpart in the interpolated and extrapolated LP, respectively, they require much shorter training time and can still achieve superior performance as reported in Table 2 and Table 3. We provide more time cost details in Appendix I.

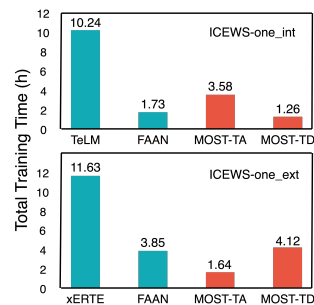


Figure 3: Training time comparison among MOST and the strongest baselines on ICEWS-based datasets.

Model	MOST-TA	MOST-TD	FAAN	TeLM	xERTE
ICEWS-one_int	0.10	0.11	35.93	0.02	-
ICEWS-one_ext	0.20	0.23	27.20	-	5.23

Table 8: Test time (min) comparison among MOST and the strongest baselines on ICEWS-based datasets.

6 Conclusion

We extend both TKG interpolated and extrapolated LP tasks to the one-shot setting, and propose a model learning meta representations of one-shot relations for solving both tasks (MOST). MOST learns meta representations from time-aware entity representations of the entities in the one-shot examples. It further employs a scoring function together with a norm regularizer for predicting missing entities. We propose four large-scale datasets, fix

the unfair evaluation settings employed by previous KG FSL methods, and compare MOST with a large group of baselines on both TKG LP tasks. Experimental results show that MOST achieves stat-of-the-art performance on both one-shot LP tasks while keeping a low time cost.

References

- Ralph Abboud, İsmail İlkan Ceylan, Thomas Lukasiewicz, and Tommaso Salvatori. 2020. [Boxe: A box embedding model for knowledge base completion](#). In *Advances in Neural Information Processing Systems 33: Annual Conference on Neural Information Processing Systems 2020, NeurIPS 2020, December 6-12, 2020, virtual*.
- Ivana Balazevic, Carl Allen, and Timothy M. Hospedales. 2019. [Tucker: Tensor factorization for knowledge graph completion](#). In *Proceedings of the 2019 Conference on Empirical Methods in Natural Language Processing and the 9th International Joint Conference on Natural Language Processing, EMNLP-IJCNLP 2019, Hong Kong, China, November 3-7, 2019*, pages 5184–5193. Association for Computational Linguistics.
- Antoine Bordes, Nicolas Usunier, Alberto García-Durán, Jason Weston, and Oksana Yakhnenko. 2013. [Translating embeddings for modeling multi-relational data](#). In *Advances in Neural Information Processing Systems 26: 27th Annual Conference on Neural Information Processing Systems 2013. Proceedings of a meeting held December 5-8, 2013, Lake Tahoe, Nevada, United States*, pages 2787–2795.
- Elizabeth Boschee, Jennifer Lautenschlager, Sean O’Brien, Steve Shellman, James Starz, and Michael Ward. 2015. [ICEWS Coded Event Data](#).
- Mingyang Chen, Wen Zhang, Wei Zhang, Qiang Chen, and Huajun Chen. 2019. [Meta relational learning for few-shot link prediction in knowledge graphs](#). In *Proceedings of the 2019 Conference on Empirical Methods in Natural Language Processing and the 9th International Joint Conference on Natural Language Processing, EMNLP-IJCNLP 2019, Hong Kong, China, November 3-7, 2019*, pages 4216–4225. Association for Computational Linguistics.
- Michaël Defferrard, Xavier Bresson, and Pierre Vandergheynst. 2016. [Convolutional neural networks on graphs with fast localized spectral filtering](#). In *Advances in Neural Information Processing Systems 29: Annual Conference on Neural Information Processing Systems 2016, December 5-10, 2016, Barcelona, Spain*, pages 3837–3845.
- Zifeng Ding, Yunpu Ma, Bailan He, and Volker Tresp. 2021. [A simple but powerful graph encoder for temporal knowledge graph completion](#). *CoRR*, abs/2112.07791.
- Zhen Han, Peng Chen, Yunpu Ma, and Volker Tresp. 2021a. [Explainable subgraph reasoning for forecasting on temporal knowledge graphs](#). In *9th International Conference on Learning Representations, ICLR 2021, Virtual Event, Austria, May 3-7, 2021*. OpenReview.net.
- Zhen Han, Zifeng Ding, Yunpu Ma, Yujia Gu, and Volker Tresp. 2021b. [Learning neural ordinary equations for forecasting future links on temporal knowledge graphs](#). In *Proceedings of the 2021 Conference on Empirical Methods in Natural Language Processing, EMNLP 2021, Virtual Event / Punta Cana, Dominican Republic, 7-11 November, 2021*, pages 8352–8364. Association for Computational Linguistics.
- Sepp Hochreiter and Jürgen Schmidhuber. 1997. [Long short-term memory](#). *Neural Comput.*, 9(8):1735–1780.
- Woojeong Jin, Meng Qu, Xisen Jin, and Xiang Ren. 2020. [Recurrent event network: Autoregressive structure inference over temporal knowledge graphs](#). In *Proceedings of the 2020 Conference on Empirical Methods in Natural Language Processing (EMNLP)*, pages 6669–6683, Online. Association for Computational Linguistics.
- Jaehun Jung, Jinhong Jung, and U Kang. 2021. [Learning to walk across time for interpretable temporal knowledge graph completion](#). In *KDD ’21: The 27th ACM SIGKDD Conference on Knowledge Discovery and Data Mining, Virtual Event, Singapore, August 14-18, 2021*, pages 786–795. ACM.
- Thomas N. Kipf and Max Welling. 2017. [Semi-supervised classification with graph convolutional networks](#). In *5th International Conference on Learning Representations, ICLR 2017, Toulon, France, April 24-26, 2017, Conference Track Proceedings*. OpenReview.net.
- Timothée Lacroix, Guillaume Obozinski, and Nicolas Usunier. 2020. [Tensor decompositions for temporal knowledge base completion](#). In *8th International Conference on Learning Representations, ICLR 2020, Addis Ababa, Ethiopia, April 26-30, 2020*. OpenReview.net.
- Julien Leblay and Melisachew Wudage Chekol. 2018. [Deriving validity time in knowledge graph](#). In *Companion of the The Web Conference 2018 on The Web Conference 2018, WWW 2018, Lyon, France, April 23-27, 2018*, pages 1771–1776. ACM.
- Kalev Leetaru and Philip A Schrodt. 2013. [Gdelt: Global data on events, location, and tone, 1979–2012](#). In *ISA annual convention*, volume 2, pages 1–49. Citeseer.
- Yankai Lin, Zhiyuan Liu, Maosong Sun, Yang Liu, and Xuan Zhu. 2015. [Learning entity and relation embeddings for knowledge graph completion](#). In *Proceedings of the Twenty-Ninth AAAI Conference on*

- Artificial Intelligence, January 25-30, 2015, Austin, Texas, USA*, pages 2181–2187. AAAI Press.
- Yunpu Ma, Volker Tresp, and Erik A. Daxberger. 2019. Embedding models for episodic knowledge graphs. *J. Web Semant.*, 59.
- Bonan Min, Ralph Grishman, Li Wan, Chang Wang, and David Gondek. 2013. Distant supervision for relation extraction with an incomplete knowledge base. In *Human Language Technologies: Conference of the North American Chapter of the Association of Computational Linguistics, Proceedings, June 9-14, 2013, Westin Peachtree Plaza Hotel, Atlanta, Georgia, USA*, pages 777–782. The Association for Computational Linguistics.
- Mehrnoosh Mirtaheri, Mohammad Rostami, Xiang Ren, Fred Morstatter, and Aram Galstyan. 2021. One-shot learning for temporal knowledge graphs. In *3rd Conference on Automated Knowledge Base Construction, AKBC 2021, Virtual, October 4-8, 2021*.
- Maximilian Nickel, Volker Tresp, and Hans-Peter Kriegel. 2011. A three-way model for collective learning on multi-relational data. In *Proceedings of the 28th International Conference on Machine Learning, ICML 2011, Bellevue, Washington, USA, June 28 - July 2, 2011*, pages 809–816. Omnipress.
- Guanglin Niu, Yang Li, Chengguang Tang, Ruiying Geng, Jian Dai, Qiao Liu, Hao Wang, Jian Sun, Fei Huang, and Luo Si. 2021. Relational learning with gated and attentive neighbor aggregator for few-shot knowledge graph completion. In *SIGIR '21: The 44th International ACM SIGIR Conference on Research and Development in Information Retrieval, Virtual Event, Canada, July 11-15, 2021*, pages 213–222. ACM.
- Adam Paszke, Sam Gross, Francisco Massa, Adam Lerer, James Bradbury, Gregory Chanan, Trevor Killeen, Zeming Lin, Natalia Gimelshein, Luca Antiga, Alban Desmaison, Andreas Köpf, Edward Z. Yang, Zachary DeVito, Martin Raison, Alykhan Tejani, Sasank Chilamkurthy, Benoit Steiner, Lu Fang, Junjie Bai, and Soumith Chintala. 2019. Pytorch: An imperative style, high-performance deep learning library. In *Advances in Neural Information Processing Systems 32: Annual Conference on Neural Information Processing Systems 2019, NeurIPS 2019, December 8-14, 2019, Vancouver, BC, Canada*, pages 8024–8035.
- Michael Sejr Schlichtkrull, Thomas N. Kipf, Peter Bloem, Rianne van den Berg, Ivan Titov, and Max Welling. 2018. Modeling relational data with graph convolutional networks. In *The Semantic Web - 15th International Conference, ESWC 2018, Heraklion, Crete, Greece, June 3-7, 2018, Proceedings*, volume 10843 of *Lecture Notes in Computer Science*, pages 593–607. Springer.
- Jiawei Sheng, Shu Guo, Zhenyu Chen, Juwei Yue, Li-hong Wang, Tingwen Liu, and Hongbo Xu. 2020. Adaptive attentional network for few-shot knowledge graph completion. In *Proceedings of the 2020 Conference on Empirical Methods in Natural Language Processing, EMNLP 2020, Online, November 16-20, 2020*, pages 1681–1691. Association for Computational Linguistics.
- Zhiqing Sun, Zhi-Hong Deng, Jian-Yun Nie, and Jian Tang. 2019. Rotate: Knowledge graph embedding by relational rotation in complex space. In *7th International Conference on Learning Representations, ICLR 2019, New Orleans, LA, USA, May 6-9, 2019*. OpenReview.net.
- Flood Sung, Yongxin Yang, Li Zhang, Tao Xiang, Philip H. S. Torr, and Timothy M. Hospedales. 2018. Learning to compare: Relation network for few-shot learning. In *2018 IEEE Conference on Computer Vision and Pattern Recognition, CVPR 2018, Salt Lake City, UT, USA, June 18-22, 2018*, pages 1199–1208. Computer Vision Foundation / IEEE Computer Society.
- Théo Trouillon, Johannes Welbl, Sebastian Riedel, Éric Gaussier, and Guillaume Bouchard. 2016. Complex embeddings for simple link prediction. In *Proceedings of the 33rd International Conference on Machine Learning, ICML 2016, New York City, NY, USA, June 19-24, 2016*, volume 48 of *JMLR Workshop and Conference Proceedings*, pages 2071–2080. JMLR.org.
- Shikhar Vashishth, Soumya Sanyal, Vikram Nitin, and Partha P. Talukdar. 2020. Composition-based multi-relational graph convolutional networks. In *8th International Conference on Learning Representations, ICLR 2020, Addis Ababa, Ethiopia, April 26-30, 2020*. OpenReview.net.
- Ashish Vaswani, Noam Shazeer, Niki Parmar, Jakob Uszkoreit, Llion Jones, Aidan N. Gomez, Lukasz Kaiser, and Illia Polosukhin. 2017. Attention is all you need. In *Advances in Neural Information Processing Systems 30: Annual Conference on Neural Information Processing Systems 2017, December 4-9, 2017, Long Beach, CA, USA*, pages 5998–6008.
- Oriol Vinyals, Charles Blundell, Tim Lillicrap, Koray Kavukcuoglu, and Daan Wierstra. 2016. Matching networks for one shot learning. In *Advances in Neural Information Processing Systems 29: Annual Conference on Neural Information Processing Systems 2016, December 5-10, 2016, Barcelona, Spain*, pages 3630–3638.
- Xiang Wang, Dingxian Wang, Canran Xu, Xiangnan He, Yixin Cao, and Tat-Seng Chua. 2019. Explainable reasoning over knowledge graphs for recommendation. In *The Thirty-Third AAAI Conference on Artificial Intelligence, AAAI 2019, The Thirty-First Innovative Applications of Artificial Intelligence Conference, IAAI 2019, The Ninth AAAI Symposium on Educational Advances in Artificial Intelligence, EAAI 2019, Honolulu, Hawaii, USA, January 27 - February 1, 2019*, pages 5329–5336. AAAI Press.

- Jiapeng Wu, Meng Cao, Jackie Chi Kit Cheung, and William L. Hamilton. 2020. [Temp: Temporal message passing for temporal knowledge graph completion](#). In *Proceedings of the 2020 Conference on Empirical Methods in Natural Language Processing, EMNLP 2020, Online, November 16-20, 2020*, pages 5730–5746. Association for Computational Linguistics.
- Wenhan Xiong, Mo Yu, Shiyu Chang, Xiaoxiao Guo, and William Yang Wang. 2018. [One-shot relational learning for knowledge graphs](#). In *Proceedings of the 2018 Conference on Empirical Methods in Natural Language Processing, Brussels, Belgium, October 31 - November 4, 2018*, pages 1980–1990. Association for Computational Linguistics.
- Chengjin Xu, Yung-Yu Chen, Mojtaba Nayeri, and Jens Lehmann. 2021. [Temporal knowledge graph completion using a linear temporal regularizer and multivector embeddings](#). In *Proceedings of the 2021 Conference of the North American Chapter of the Association for Computational Linguistics: Human Language Technologies, NAACL-HLT 2021, Online, June 6-11, 2021*, pages 2569–2578. Association for Computational Linguistics.
- Chengjin Xu, Mojtaba Nayeri, Fouad Alkhoury, Jens Lehmann, and Hamed Shariat Yazdi. 2019. [Temporal knowledge graph embedding model based on additive time series decomposition](#). *CoRR*, abs/1911.07893.
- Da Xu, Chuanwei Ruan, Evren Körpeoglu, Sushant Kumar, and Kannan Achan. 2020. [Inductive representation learning on temporal graphs](#). In *8th International Conference on Learning Representations, ICLR 2020, Addis Ababa, Ethiopia, April 26-30, 2020*. OpenReview.net.
- Bishan Yang, Wen-tau Yih, Xiaodong He, Jianfeng Gao, and Li Deng. 2015. [Embedding entities and relations for learning and inference in knowledge bases](#). In *3rd International Conference on Learning Representations, ICLR 2015, San Diego, CA, USA, May 7-9, 2015, Conference Track Proceedings*.
- Chuxu Zhang, Huaxiu Yao, Chao Huang, Meng Jiang, Zhenhui Li, and Nitesh V. Chawla. 2020. [Few-shot knowledge graph completion](#). In *The Thirty-Fourth AAAI Conference on Artificial Intelligence, AAAI 2020, The Thirty-Second Innovative Applications of Artificial Intelligence Conference, IAAI 2020, The Tenth AAAI Symposium on Educational Advances in Artificial Intelligence, EAAI 2020, New York, NY, USA, February 7-12, 2020*, pages 3041–3048. AAAI Press.
- Yuyu Zhang, Hanjun Dai, Zornitsa Kozareva, Alexander J. Smola, and Le Song. 2018. [Variational reasoning for question answering with knowledge graph](#). In *Proceedings of the Thirty-Second AAAI Conference on Artificial Intelligence, (AAAI-18), the 30th innovative Applications of Artificial Intelligence (IAAI-18), and the 8th AAAI Symposium on Educational Advances in Artificial Intelligence (EAAI-18), New Orleans, Louisiana, USA, February 2-7, 2018*, pages 6069–6076. AAAI Press.
- Cunchao Zhu, Muhao Chen, Changjun Fan, Guangquan Cheng, and Yan Zhang. 2021. [Learning from history: Modeling temporal knowledge graphs with sequential copy-generation networks](#). In *Thirty-Fifth AAAI Conference on Artificial Intelligence, AAAI 2021, Thirty-Third Conference on Innovative Applications of Artificial Intelligence, IAAI 2021, The Eleventh Symposium on Educational Advances in Artificial Intelligence, EAAI 2021, Virtual Event, February 2-9, 2021*, pages 4732–4740. AAAI Press.

Appendix

A Related Work

Knowledge Graph Embedding Methods

Knowledge graph embedding (KGE) methods serve as a key driver for KG reasoning tasks, e.g., KG link prediction. A line of KGE methods are developed aiming to solve static KG reasoning tasks by designing novel scoring functions that are used to compute the plausibility scores of KG facts (Bordes et al., 2013; Lin et al., 2015; Trouillon et al., 2016; Sun et al., 2019). Due to the success of graph neural networks (GNNs) (Defferrard et al., 2016; Kipf and Welling, 2017), another group of methods spend great effort on developing neural-based relational graph encoders for KG representation learning (Schlichtkrull et al., 2018; Vashishth et al., 2020), which helps to learn more expressive graph embeddings by utilizing structural information of KGs. With the combination of GNN-based graph encoders and existing KG scoring functions, these methods show strong effectiveness on KG reasoning tasks.

Temporal Knowledge Graph Embedding Methods

In recent years, an increasing interest has shown in developing temporal KGE methods for TKGs. Many existing methods derive time-aware KG scoring functions (Leblay and Chekol, 2018; Ma et al., 2019; Lacroix et al., 2020), while another series of methods employ recurrent modules to autoregressively encode temporal dependencies between TKG events (Jin et al., 2020; Wu et al., 2020; Han et al., 2021b). Apart from them, it has been proven to be effective to sample temporal neighboring graph for TKG entities and learn contextualized time-aware entity representations (Han et al., 2021a; Jung et al., 2021; Ding et al., 2021). By

considering temporal information, temporal KGE methods outperform static KGE methods in TKG reasoning tasks, e.g., TKG completion.

Few-shot Relational Learning Methods for Knowledge Graphs

To alleviate the impact of the KG incompleteness problem on the performance of KGE methods, Xiong et al. (Xiong et al., 2018) propose a meta-learning based method Gmatching as the first work introducing few-shot relational learning into the context of KG. (Chen et al., 2019) follows the meta-learning framework and proposes MetaR which transfers relation-specific meta information to the sparse relations. Based on Gmatching, FSRL (Zhang et al., 2020) presents a recurrent autoencoder aggregation layer to better extract information from the few-shot examples, thus achieving stronger performance with the increasing few-shot size. FAAN (Sheng et al., 2020) further employs an adaptive attentional network as the neighbor encoder and learns adaptive query-aware entity representations, which helps to better differentiate supporting information from entities’ neighborhoods. Similar to FAAN, GANA (Niu et al., 2021) presents a gated attentional aggregator for learning contextualized entity representations. A novel MTransH scoring function is designed for modeling complex relations and it contributes greatly to the model performance.

OAT (Mirtaheri et al., 2021) is the first method developed for one-shot relational learning for TKGs. A Transformer-based (Vaswani et al., 2017) history encoder is employed to encode historical information and generate time-aware entity representations. Coupled with a multi-layer feed forward neural network, entity representations of the one-shot example are used to compute the plausibility scores of TKG facts. In this work, Mirtaher et al. propose an extrapolation LP task for TKGs in the one-shot setting, together with two datasets constructed from the subsets of two benchmark TKG databases, i.e., ICEWS (Boschee et al., 2015) and GDELT (Leetaru and Schrod, 2013).

B One-shot Temporal Knowledge Graph Extrapolation Setting

C Evaluation Protocol

For each test quadruple $(s_q, r_q, o_q, t_q) \in \mathcal{Q}_r$, $r_q \in \mathcal{R}_{sp}^{test}$, we derive two link prediction queries: $(s_q, r_q, ?, t_q)$ and $(?, r_q, o_q, t_q)$. Following (Han

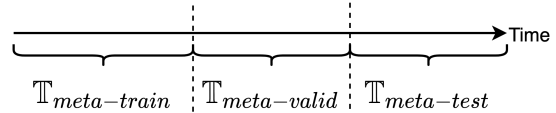


Figure 4: Time span of meta-learning sets ($\mathbb{T}_{meta-train}, \mathbb{T}_{meta-valid}, \mathbb{T}_{meta-test}$) for the extrapolated LP. There exist no time overlap between every two of them.

et al., 2021a), we transform $(?, r_q, o_q, t_q)$ into $(o_q, r^{-1}, ?, t_q)$ (r^{-1} denotes the reciprocal relation of r), and perform object prediction. We compute the rank of the ground truth missing entities (s_q or o_q) for every link prediction query. Let ψ_{s_q} and ψ_{o_q} denote the rank of $(?, r_q, o_q, t_q)$ and $(s_q, r_q, ?, t_q)$, respectively. We compute MRR by averaging the ranks among all the test quadruples:

$$\frac{1}{\sum_{r_q \in \mathcal{R}_{sp}^{test}} 2|\mathcal{Q}_{r_q}|} \sum_{r_q \in \mathcal{R}_{sp}^{test}} \sum_{\tilde{q} \in \mathcal{Q}_{r_q}} \left(\frac{1}{\psi_{s_q}} + \frac{1}{\psi_{o_q}} \right), \quad (7)$$

where \tilde{q} denotes a test quadruple (s_q, r_q, o_q, t_q) . Hits@1/3/5/10 are the proportions of the predicted links where ground truth entities are ranked as top 1, top 3, top 5, top 10, respectively.

D Implementation Details

We implement all experiments with PyTorch (Paszke et al., 2019) on a single NVIDIA Tesla T4. We use the hyperparameter searching strategy stated in Table 9. For every dataset, we do 648 trials, and let our model run for 10000 batches. We select the trial leading to the best performance on the meta-validation set and take this hyperparameter setting as our best configuration. We train our model five times and report averaged results. The best hyperparameter settings are reported in Table 13. The GPU memory usage is reported in Table 12. We also report the validation results of both TKG one-shot LP tasks in Table 10 and Table 11.

For baseline methods, we use the official implementation of TNTComplex¹, ATiSE², TeLM³, TANGO⁴, CyGNet⁵, xERTE⁶, GMatching⁷,

¹<https://github.com/facebookresearch/tkbc>

²<https://github.com/soledad921/ATiSE>

³<https://github.com/soledad921/TeLM>

⁴<https://github.com/TemporalKGTeam/TANGO>

⁵<https://github.com/CunchaoZ/CyGNet>

⁶<https://github.com/TemporalKGTeam/xERTE>

⁷<https://github.com/xwhan/One-shot-Relational-Learning>

MetaR ⁸, FSRL ⁹, FAAN ¹⁰, GANA ¹¹, and OAT ¹². We pretrain Dismult (Yang et al., 2015) on the whole background graph of every interpolation dataset, and on the background graph before the end of meta-training set of every extrapolation dataset. We initialize the entity representations of KG FSL methods with the pretrained embeddings. We provide the hyperparameter settings of all baseline methods in Table 14 and Table 15. We refer to the best hyperparameter settings of baseline methods reported in their original papers.

Hyperparameter	Search Space
Time Encoding Strategy	{TA, TD}
Embedding Size	{50, 100, 200}
# Aggregation Step	{1, 2}
Activation Function	{Tanh, ReLU, LeakyReLU}
Dropout	{0.2, 0.3, 0.5}
# Temporal Neighbor	{64, 128, 512}
Batch Size	{64, 128}

Table 9: Hyperparameter searching strategy.

E Discussion about Unfair Evaluation for Static KG FSL Methods

Collapsing a TKG into an unweighted static KG will cause unfair evaluation for static KG FSL methods. For example, in the original TKG, there exist n identical events $\{(Xi Jinping, host a visit, Angela Merkel, t_1), \dots, (Xi Jinping, host a visit, Angela Merkel, t_n)\}$ that happen at n different timestamps. If n is a large number, these n repeated events will introduce a strong inductive bias showing that the entities, *Xi Jinping* and *Angela Merkel*, are likely to be highly correlated. Collapsing the original TKG into an unweighted static KG will lose great amounts of information for static KG FSL methods, and force the models to learn more from weakly correlated entities.

To empirically prove our assertion, we collapse our datasets into unweighted static KGs and rerun all static KG FSL methods on them. We retrain Dismult on the unweighted background graphs for embedding initialization. We report the experimental results in Table 16 and Table 17. By comparing with Table 2 and Table 3, we observe that in most

cases, collapsing TKGs into unweighted KGs worsens the performance of static KG FSL methods greatly.

F Model Analysis

We provide the justification about why our model outperforms baseline methods. For traditional TKG embedding methods, i.e., TNTComplex, ATiSE, TeLM, TANGO, CyGNet, xERTE, they are not designed to capture meta information from one-shot examples and further generalize to the examples concerning sparse relations. They are more prone to learn from frequent relations since they do not employ a meta-learning framework. For static KG FSL methods, i.e., Gmatching, MetaR, FSRL, FAAN, GANA, they do not incorporate temporal information, thus underperforming in both LP tasks. The TKG FSL method OAT is designed for extrapolated LP. It includes temporal information by employing a snapshot encoder that sequentially encodes a fixed number of historical graph snapshots right before the query timestamp. For the interpolation task, OAT loses the temporal information coming after the query timestamp, which causes degenerated performance. For the extrapolation task, a fixed history length is not long enough to include enough temporal information. In our work, we search for the nearest temporal neighbors in our graph encoder and do not impose constraint on how far away these neighbors are. This helps to incorporate temporal neighbors in a better way. Besides, OAT employs cosine similarity for score computation, which is beaten by the scoring function presented in our meta-relational decoder. Another point worth noting is that OAT performs much worse on ICEWS-based datasets (Table 2 and Table 3). It is due to the characteristics of databases. As discussed in (Wu et al., 2020), ICEWS database is much sparser than GDELT. This implies that by only considering a fixed number of previous snapshots, it is less likely to capture enough historical information, which causes worse performance on ICEWS-based datasets.

G Further Analysis of Previous Datasets

We do an analysis on ICEWS17 and GDELT proposed in (Mirtaheeri et al., 2021). In ICEWS17, 31 out of 85 sparse relations have less than 50 associated quadruples. In GDELT, 24 out of 69 sparse relations have less than 50 associated quadruples. Moreover, 4 out of 14 test relations have even less

⁸<https://github.com/AnselCmy/MetaR>

⁹https://github.com/chuxuzhang/AAAI2020_FSRL

¹⁰<https://github.com/JiaweiSheng/FAAN>

¹¹<https://github.com/ng1567/GANA-FewShotKGC>

¹²<https://openreview.net/forum?id=GF8wO8MFQOR>

Datasets	ICEWS-one_int					GDELT-one_int				
Model	MRR	Hits@1	Hits@3	Hits@5	Hits@10	MRR	Hits@1	Hits@3	Hits@5	Hits@10
MOST-TA	39.76	30.63	44.79	49.44	56.35	14.92	9.03	16.12	20.03	25.96
MOST-TD	41.00	32.11	45.05	49.47	57.40	15.14	9.39	16.29	20.36	26.51

Table 10: Validation results of MOST on interpolated LP datasets. Evaluation metrics are filtered MRR and Hits@1/3/5/10 (%).

Datasets	ICEWS-one_ext					GDELT-one_ext				
Model	MRR	Hits@1	Hits@3	Hits@5	Hits@10	MRR	Hits@1	Hits@3	Hits@5	Hits@10
MOST-TA	24.21	14.81	26.69	34.05	43.93	12.49	7.88	12.92	15.92	20.92
MOST-TD	38.20	31.09	40.65	45.89	52.45	14.55	9.32	15.34	19.12	22.26

Table 11: Validation results of MOST on extrapolated LP datasets. Evaluation metrics are filtered MRR and Hits@1/3/5/10 (%).

Datasets	ICEWS-one_ext	ICEWS-one_int	GDELT-one_ext	GDELT-one_int
Model	GPU Memory	GPU Memory	GPU Memory	GPU Memory
MOST-TA	3327MB	3327MB	2967MB	2545MB
MOST-TD	5759MB	3327MB	3315MB	2967MB

Table 12: GPU memory usage.

Datasets	ICEWS-one_ext	ICEWS-one_int	GDELT-one_ext	GDELT-one_int
Hyperparameter				
Time Encoding Strategy	TD	TA	TD	TA
Embedding Size	200	100	100	50
# Aggregation Step	1	1	1	1
Activation Function	ReLU	ReLU	LeakyReLU	LeakyReLU
Dropout	0.2	0.2	0.3	0.3
# Temporal Neighbor	512	512	512	512
Batch Size	64	64	64	64

Table 13: Best hyperparameter settings on each dataset.

than 10 associated quadruples in ICEWS17, and this also applies for 11 out of 14 test relations in GDELT. In the first work (Xiong et al., 2018) who proposes few-shot relational learning for KGs, all the relations whose frequencies are lower than the lower threshold are removed in the datasets to keep sufficient test examples. We follow this tradition and propose large-scale datasets that fix the problem from (Mirtaheeri et al., 2021) in the context of one-shot relational learning for TKGs.

H Performance over Different Relations on GDELT-based Datasets

We compare MOST with FAAN over different sparse relations on GDELT-based datasets. Table 18 and Table 19 show that MOST achieves significant improvement in LP concerning most sparse relations.

I Time Cost Analysis Details

Similar to Figure 3, in Figure 5, we report the total training time comparison among MOST and several strong baselines on GDELT-one_int and GDELT-one_ext. Note that static KG FSL methods

Datasets	ICEWS-one_int			GDELT-one_int		
	Embedding Size	# Negative Sample	Batch Size	Embedding Size	# Negative Sample	Batch Size
TNTComplEx	256	-	1000	312	-	1000
ATiSE	500	10	512	500	10	512
TeLM	4000	-	1000	4000	-	1000
GANa	100	1	1024	100	1	1024
MetaR	100	1	1024	100	1	1024
GMatching	100	1	128	100	1	128
FSRL	100	1	128	100	1	128
FAAN	100	1	128	100	1	128
OAT	50	1	100	50	1	100

Table 14: Hyperparameter settings of interpolation baselines.

Datasets	ICEWS-one_ext			GDELT-one_ext		
	Embedding Size	# Negative Sample	Batch Size	Embedding Size	# Negative Sample	Batch Size
TANGO	200	-	-	200	-	-
CyGNet	200	-	1024	200	-	1024
xERTE	256	-	128	128	-	128
GANa	100	1	1024	100	1	1024
MetaR	100	1	1024	100	1	1024
GMatching	100	1	128	100	1	128
FSRL	100	1	128	100	1	128
FAAN	100	1	128	100	1	128
OAT	50	1	100	50	1	100

Table 15: Hyperparameter settings of extrapolation baselines.

employ pretrained KG embeddings for initialization. We do not include this time cost into the numbers presented in Figure 3 and Figure 5. MOST does not require pretraining and it also keeps low time cost while training GDELT-based datasets. Except for training time, evaluation time is also a critical factor affecting the total time cost of model development. We report evaluation time of all methods on meta-test sets in Table 20 and Table 21. We find that MOST keeps extremely low time consumption during evaluation. This greatly accelerates the process of model development.

We attribute the high training time efficiency of MOST to the employment of binary cross entropy loss. We treat every entity other than the ground truth missing entity as a negative sample, rather than sampling a number of negative samples for each LP query. We avoid the time cost during sampling and we also jointly learn the representations of all entities when we perform prediction for every LP query. For evaluation, during score computation, we do not compute contextualized entity representations for all candidates. Instead, we incorporate temporal information with a simple time encoding layer for all the entities together. Some of previous methods, e.g., OAT, compute the score for

each candidate entity by going through the whole model (e.g. going through the whole model for $|\mathcal{E}|$ times if there exist $|\mathcal{E}|$ entities). However, in our work, we only need to go through the whole model for one time, thus cutting great time cost during evaluation.

J Data Construction Process

Interpolation Datasets

1. We take ICEWS05-15¹³ and GDELT¹⁴ as the databases for dataset construction.
2. For each database, by tracking every relation’s frequency of occurrence, we divide all relations into two groups, i.e., frequent relations and sparse relations. Relations occurring between 50 and 500 times in ICEWS05-15, and 100 and 1000 times for GDELT are taken as sparse relations. Those occurring more than 500 times in ICEWS05-15 and more than 1000 times in GDELT are considered as frequent relations.
3. For each database, the quadruples contain-

¹³<https://github.com/mniepert/mmkbtree/master/TemporalKGs>

¹⁴<https://github.com/INK-USC/RE-Net/tree/master/data>

Datasets	ICEWS-one_int					GDELT-one_int				
	MRR	Hits@1	Hits@3	Hits@5	Hits@10	MRR	Hits@1	Hits@3	Hits@5	Hits@10
GANA	9.49	3.14	12.74	16.27	21.47	5.08	2.86	5.08	6.32	9.12
MetaR	17.73	0.00	28.96	38.77	49.13	7.94	0.11	10.41	14.99	22.14
GMatching	21.63	10.44	24.36	33.34	45.52	11.61	5.98	11.61	15.41	22.43
FSRL	21.09	9.90	23.99	32.34	43.84	11.08	5.67	11.12	14.61	21.32
FAAN	23.05	11.95	26.87	34.76	45.84	12.62	6.66	13.42	16.82	23.72

Table 16: Interpolated LP results on collapsed unweighted KGs. Evaluation metrics are filtered MRR and Hits@1/3/5/10 (%).

Datasets	ICEWS-one_ext					GDELT-one_ext				
	MRR	Hits@1	Hits@3	Hits@5	Hits@10	MRR	Hits@1	Hits@3	Hits@5	Hits@10
GANA	17.10	5.55	22.84	29.28	38.88	9.75	0.69	13.31	18.26	25.48
MetaR	15.28	2.46	21.74	29.35	39.98	8.11	0.08	11.23	15.61	26.30
GMatching	15.99	8.29	16.97	22.90	32.99	11.82	7.27	11.44	14.67	22.24
FSRL	11.96	5.62	10.63	16.32	26.54	9.69	7.21	9.09	10.93	14.17
FAAN	19.51	11.31	21.94	27.50	34.56	12.81	7.80	13.02	16.25	21.28

Table 17: Extrapolated LP results on collapsed unweighted KGs. Evaluation metrics are filtered MRR and Hits@1/3/5/10 (%).

GDELT-one_int		MRR		Hits@10	
CAMEO	Frequency	MOST-TA	FAAN	MOST-TA	FAAN
0861	108	35.94	9.52	60.28	17.75
1722	167	9.46	11.54	16.26	18.37
185	177	12.23	7.65	22.72	15.05
0862	234	17.07	15.13	26.82	19.14
1044	411	14.16	7.00	24.75	17.07
133	675	18.21	13.77	31.67	26.18
0871	748	19.65	13.41	31.59	29.18
139	752	17.98	16.84	30.15	26.36

Table 18: Performance over each sparse relation in GDELT-one_int. CAMEO denotes the CAMEO code for each relation. The best results are marked in bold.

ing its frequent relations form the background graph \mathcal{G}' . We split its sparse relations into meta-train/meta-valid/meta-test groups, and the quadruples containing the sparse relations are kept for meta-learning process.

Extrapolation Datasets

1. We take ICEWS05-15 and GDELT as the databases for dataset construction.
2. For each database, by tracking every relation’s frequency of occurrence, we divide all relations into two groups, i.e., frequent relations and sparse relations. Relations occurring between 100 and 1000 times in ICEWS05-15, and 200 and 2000 times for GDELT are taken as sparse relations. Those occurring more than 1000 times in ICEWS05-15 and more

GDELT-one_ext		MRR		Hits@10	
CAMEO	Frequency	MOST-TD	FAAN	MOST-TD	FAAN
91	149	15.34	15.90	19.25	22.97
0356	153	19.58	15.83	33.55	28.28
037	160	22.19	8.01	33.64	14.46
145	176	18.72	11.66	28.00	24.00
1831	180	10.17	5.06	17.31	15.08
171	212	17.04	11.43	27.01	17.06
129	279	22.78	23.15	34.71	38.12
1014	312	14.75	15.61	27.00	26.20
140	321	15.67	10.21	26.71	25.46
0231	348	15.21	16.17	23.77	24.06
0331	359	19.69	17.67	30.02	23.74

Table 19: Performance over each sparse relation in GDELT-one_ext. CAMEO denotes the CAMEO code for each relation. The best results are marked in bold.

than 2000 times in GDELT are considered as frequent relations.

3. For each database, the quadruples containing its frequent relations form the background graph \mathcal{G}' . We split sparse relations into meta-train/meta-valid/meta-test groups, and remove a number of quadruples to avoid time overlap between every two of sparse relation groups (following (Mirtaheri et al., 2021)). After quadruple removal, if the number of a sparse relation’s associated quadruples is smaller than 50 for ICEWS, 100 for GDELT, we discard all the quadruples concerning this sparse relation. The remaining quadruples containing sparse relations are kept for meta-

learning process.

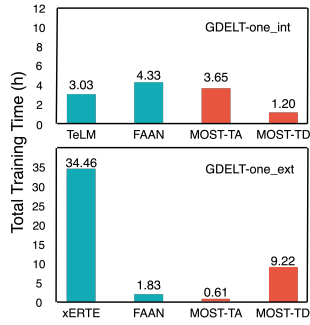


Figure 5: Training time comparison among MOST and the strongest baselines on GDELT-one_int and GDELT-one_ext.

Datasets	ICEWS-one_int	GDELT-one_int
Model		
TNTComplex	0.02	0.03
ATiSE	2.20	2.77
TeLM	0.02	0.04
GANa	9.77	11.12
MetaR	8.01	7.33
GMatching	52.31	43.23
FSRL	32.21	23.66
FAAN	35.93	41.08
OAT	612.34	781.49
MOST-TA	0.10	0.27
MOST-TD	0.11	0.24

Table 20: Test time (min) comparison of all methods on interpolation datasets.

Datasets	ICEWS-one_ext	GDELT-one_ext
Model		
TANGO	3.76	4.54
CyGNet	1.68	5.56
xERTE	5.23	12.41
GANa	3.64	7.86
MetaR	4.13	8.99
GMatching	19.61	18.91
FSRL	10.06	18.28
FAAN	27.20	33.78
OAT	1112.17	1507.78
MOST-TA	0.20	0.29
MOST-TD	0.23	0.46

Table 21: Test time (min) comparison of all methods on extrapolation datasets.